Appl. Phys. B 71, 853–857 (2000) / Digital Object Identifier (DOI) 10.1007/s003400000431

Applied Physics B
Lasers
and Optics

Simultaneous detection of methane, oxygen and water vapour utilising near-infrared diode lasers in conjunction with difference-frequency generation

U. Gustafsson, J. Sandsten, S. Svanberg

Department of Physics, Lund Institute of Technology, P.O. Box 118, 22100 Lund, Sweden
(Fax: +46-46/222-4250, E-mail: sune.svanberg@fysik.lth.se)

Received: 6 March 2000/Revised version: 19 June 2000/Published online: 11 October 2000 –

Abstract. An all-diode-laser-based spectrometer is used for the simultaneous detection of methane, oxygen and water vapour. This is accomplished using a 760-nm diode laser and a 980-nm diode laser in conjunction with difference-frequency generation to 3.4 μm in a periodically poled lithium niobate crystal. Each of the output wavelengths is resonant with one of the molecular species. Simultaneous recordings over a 15-m open path of laboratory air are demonstrated. The recording scheme shows the wide applicability of a diode-laser-based difference-frequency spectrometer for the detection of molecular species in different wavelength ranges. By increasing the frequency of the 760-nm diode laser and decreasing the frequency of the 980-nm diode laser, a maximum continuous tuning range in the mid infrared of 3.6 cm^{-1} is achieved. This enables the recording of several methane lines at atmospheric pressure. Pressure-dependence studies of methane lineshapes are also performed in an absorption cell. An indoor-air methane background level of 3 ppm is measured. The signal-to-noise ratio in the recorded methane spectra indicates that sub-ppm detection of methane at atmospheric pressure is feasible.

PACS: 42.55.Px; 42.62.Fi; 42.65.Ky

Laser absorption spectroscopy is a powerful technique for fast and sensitive detection of many gases in e.g. atmospheric monitoring, process control and combustion diagnostics. The technique has been widely employed in the mid-infrared spectral region (2–15 μm), where numerous species of interest have strong fundamental vibrational absorption bands, and in the near-infrared region (0.6–2 μm), where weaker overtone and combination bands occur. Available laser sources in the mid-infrared region, e.g. lead-salt diode lasers, colour-centre lasers and CO or CO_2 lasers, each suffer from various practical drawbacks such as the need for cryogenic cooling, limited tuning range, poor amplitude and frequency stability, large size, high cost or high power consumption. The promising and newly developed but not yet commercially available quantum-cascade lasers have been used in spectroscopic investigations in the infrared [1–3], but continuous-wave operation requires cryogenic cooling and rather high supply voltages. In the near-infrared region, on the other hand, diode-laser technology offers several hundred milliwatts of narrow-band tuneable radiation at room temperature from small and low-cost devices. Using these near-infrared diode lasers and/or compact high-power diode-pumped solid-state lasers, great efforts have been made during the last few years in developing difference-frequency generation (DFG) in non-linear materials for trace-gas detection using the mid-infrared absorption bands [4–13].

All DFG implementations have so far only focused on the spectroscopic use of the generated mid-infrared radiation, disregarding the possibility of also using the generating laser wavelengths for probing the absorption bands in the near-infrared region. In the present study we explore simultaneous detection of atmospheric oxygen at 760 nm, water vapour at 980 nm and methane at 3.4 μm using near-infrared lasers in conjunction with difference-frequency mixing in a periodically poled lithium niobate (PPLN) crystal. Such simultaneous detection of interacting species is frequently of great interest, e.g. in connection with combustion. Certain important molecules, such as oxygen, can be detected in the near-infrared region but do not have strong mid-infrared absorption.

Actually, a similar use of coincidences of excitation spectra occurring in sum-frequency mixing of pulsed dye laser radiation has been used to simultaneously induce fluorescence in the important flame species OH, NO and O (two-photon excitation) [14] and in HN_3, OH and NO [15]. More cumbersome, simultaneous O_2, H_2O and temperature measurements have been performed by individually scanning three different near-infrared diode lasers [16], just as simultaneous flame-fluorescence imaging of C_2 and OH could be achieved with independent laser systems [17]. Alternatively, simultaneous fluorescence detection of flame species can be achieved when absorption lines are inter-mingled in a certain spectral region, such as for OH, NH, CH and CN around 312.2 nm [18]. Similarly, in the mid-infrared region, where difference-frequency

mixing has been used for absorption measurements, CH_4 and H_2O could be detected around 3.4 μm [8, 11], CH_4 and H_2CO around 3.5 μm [10], CO_2 and N_2O around 4.4 μm [9], or CO and H_2O around 4.8 μm [12].

1 Experimental set-up

Our experimental set-up is schematically illustrated in Fig. 1. The two Fabry–Perot-type diode lasers (Laser Components Specdilas F760 and Power Technology LD1313), operating around 760 nm and 980 nm and having a maximum output power of 55 mW and 200 mW, respectively, are placed in thermoelectrically cooled mounts. Temperature and current are controlled by low-noise diode-laser drivers (Melles Griot 06DLD103). Coarse wavelength tuning of the diode lasers is accomplished by changing the temperature around the diode-laser capsules between 10 °C and 40 °C, resulting in a tuning range of about 5 nm for the 760-nm diode laser and of 8 nm for the 980-nm diode laser. Fine tuning is accomplished by changing the diode-laser currents. Wavelength scanning is made by adding a 110-Hz current ramp (Hewlett-Packard 33120A) to the operating current of one or both of the two diode lasers.

The vertically polarised diode-laser outputs are first collimated by anti-reflection-coated moulded-glass aspherical lenses (Geltech C230TM-B), and the elliptical beam profiles are then made circular by two anamorphic prism pairs (Melles Griot 06GPA004). The two collimated and circular beams are spatially overlapped in a dichroic beamsplitter (Melles Griot 88NPDC875) and focused by an 8.5-cm focal length achromatic lens into the PPLN crystal (Crystal Technologies 97-02355-01). The focusing into the crystal was simulated with a ray-tracing program (Sinclair Optics OSLO) to choose an optimal lens. The 19-mm long and 0.5-mm thick PPLN crystal without antireflection coating has 10 grating periods, each 1-mm wide, between 18.6 μm and 20.4 μm in 0.2 μm increments. A crystal oven (Super Optronics OTC-PPLN-20) ensures stable temperature of the PPLN crystal and fine tuning of the grating period for proper phase matching.

After the PPLN crystal, the two near-infrared beams and the generated mid-infrared beam are collimated by a 10-cm focal length CaF_2 lens, and then transmitted through approximately 15 m of laboratory air in a common open path. An anti-reflection-coated germanium filter is used as a beamsplitter, to reflect the near-infrared radiation and transmit the mid-infrared radiation. A CaF_2 lens with a focal length of 10 cm focuses the mid-infrared beam onto a thermoelectrically cooled HgCdZnTe detector (Boston Electronics PDI-2TE-5) with an active area of 1 mm^2 and an immersed focusing lens. Combining an external focusing lens and a detector with an immersed lens simplifies the positioning of the small-area detector. A glass prism separates the two near-infrared wavelengths, and the intensities are detected by two pin photodiodes (Hamamatsu S-5821). The mid-infrared beam is in some of the experiments directed through a 10-cm long absorption cell with wedged CaF_2 windows for high-resolution measurements at low pressures and studies of pressure broadening.

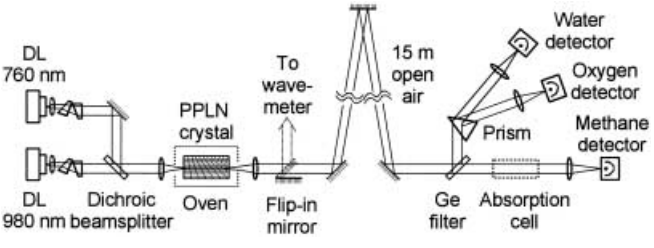

Fig. 1. Experimental set-up for simultaneous ambient-air monitoring of O_2, H_2O and CH_4

The detected signals are amplified and low-pass filtered at 30 kHz in low-noise preamplifiers (Stanford SRS560) and viewed in real-time on two-channel digitising oscilloscopes (Tektronix TDS520B). The data are then transferred to a computer for processing and evaluation. A germanium etalon with a free spectral range of 0.05 cm^{-1} can be inserted in the mid-infrared beam for relative frequency calibration, and a glass etalon with a free spectral range of 0.08 cm^{-1} can likewise be used for the near-infrared beams. A flip-in mirror is used to redirect the two diode-laser beams to a wavemeter (Burleigh WA-4500) for precise measurements of the diode-laser wavelengths at different temperature and current settings.

No optical isolators are used in the experiments. Instead, all optics are placed with a small angle to the laser beams to avoid optical feedback. Especially important is to angle (1 to 2° is sufficient) the PPLN crystal, since placing it exactly perpendicular to the input beams resulted in severe optical feedback to both diode lasers. Another important factor is the immersed lens on the mid-infrared detector. Tests using a detector without an immersed lens also showed significant instabilities in the output spectra of the two diode lasers. The tilting scheme probably means that we have a somewhat less than optimum conversion efficiency in the PPLN crystal due to a slight beam walk-off, but it also has the added benefit of reducing etalon effects, often encountered in infrared absorption experiments, to a minimum.

The simplest and most often used tuning method in the mid infrared utilising difference-frequency generation is achieved by changing the wavelength of one laser, while the wavelength of the other laser is fixed. The tuning range in the mid infrared is then limited by the maximum tuning range of only one laser. Alternatively, both lasers can be tuned synchronously, resulting in a very large tuning range in the mid infrared. By temperature tuning of the two near-infrared diode lasers a theoretical mid-infrared tuning range of about 170 cm^{-1} is possible (from 2895 cm^{-1} to 3065 cm^{-1}). Due to the mode-jump behaviour of all Fabry–Perot-type diode lasers, some regions will not be accessible. We have investigated some regions in this range, and once a region of interest was established by temperature tuning, we applied the finer and much faster current tuning. In the experiments we use both of the near-infrared diode lasers for molecular spectroscopy and therefore they are driven by current ramps. Depending on the relative scan directions, a long or a short mid-infrared scan can be achieved. By increasing the frequency of the high-frequency diode laser (760 nm) with a negative current ramp and decreasing the frequency of the low-frequency diode laser (980 nm) with a positive current ramp, a maximum continuous tuning range in the mid infrared of 3.6 cm^{-1} has been achieved. A recording of the germanium-etalon fringes during such a scan is shown in

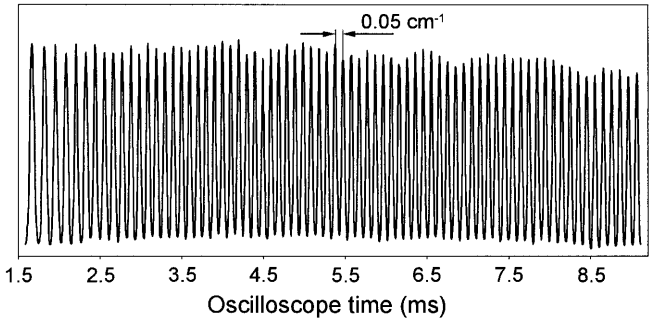

Fig. 2. Ge etalon fringes around 3.4 μm corresponding to a continuous tuning range of 3.6 cm^{-1} (72 fringes)

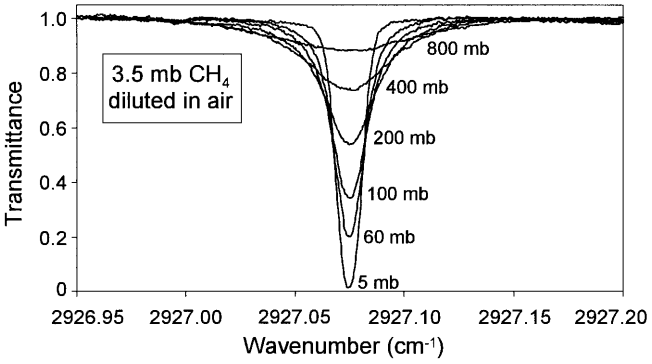

Fig. 3. Methane spectrum as a function of pressure at 3.42 μm. The recordings are 500-scan averages, corresponding to a total sampling time of 4.5 s for each curve

Fig. 2. By changing scan directions, very short frequency scans are possible and, in principle, it is also possible to fix the mid-infrared frequency.

With near-infrared input powers of $P_1 = 45$ mW and $P_2 = 195$ mW at 760 nm and 980 nm, respectively, a maximum mid-infrared power of about 9 μW at 3.4 μm was generated. From the theory of difference-frequency mixing of focused Gaussian beams, the mid-infrared power can be expressed by [19]

$$P_3 = \frac{4\omega_3 d_{\text{eff}}^2 l}{\pi\varepsilon_0 c n_1 n_2 n_3 (k_1^{-1} + k_2^{-1})} h\left(\frac{k_2}{k_1}, \frac{l}{b}\right) T P_1 P_2 \,, \tag{1}$$

where

$$h(\mu, \xi) = \frac{1}{2\xi} \int_{-\xi}^{\xi} \mathrm{d}\tau \int_{0}^{\xi} \mathrm{d}\tau' \frac{1 + \tau\tau'}{(1+\tau\tau')^2 + \left(\frac{1+\mu^2}{1-\mu^2}\right)^2 (\tau - \tau')^2} \,. \tag{2}$$

Here the subscripts $i = 1$, 2 and 3 refer to the beams at 760 nm, 980 nm and 3.4 μm, respectively, n_i are the refractive indices of the PPLN crystal, P_i are the powers, k_i are the wave vectors, ω_i are the angular frequencies, $d_{\text{eff}} = (2/\pi) \times 27$ pm/V is the effective non-linear coefficient, l is the crystal length, $b = 10$ mm is the confocal parameter of the two mode-matched input beams, $T = 65\%$ accounts for the reflection losses at the crystal input and output facets, μ is the ratio of the input wave vectors (k_2/k_1), ξ is the ratio of the crystal length and the confocal parameter, c is the speed of light and ε_0 is the permittivity of free space. Inserting our experimental values, we calculate a theoretical mid-infrared power of $P_3 = 11.8$ μW. The deviation between measured and calculated mid-infrared powers can most likely be ascribed to our inclination of the PPLN crystal.

2 Spectroscopic studies

Studies of the absorption spectrum of methane were performed with the generated mid-infrared beam passing through the 10-cm absorption cell. Recordings of a methane line from the P-branch of the ν_3 band at 2927.075 cm^{-1} are shown in Fig. 3 for 3.5 mbar of pure methane in a total pressure of 5 mbar; this methane concentration is then successively diluted by air up to 800 mbar. In these recordings only the 760-nm diode laser was scanned. We observe a line broadening from 390 MHz to 2.4 GHz, corresponding to a pressure-broadening coefficient of 2.6 MHz/mbar, in good agreement with previous results [20]. The laser-system linewidth was estimated to be 280 MHz with a CH_4 Doppler linewidth of 270 MHz and the observed lowest linewidth of 390 MHz. We note that a very good signal-to-noise ratio is achievable, allowing sensitive trace-gas detection at low pressures. At atmospheric pressure the lines broaden and overlap, and it is impossible to distinguish the weak transitions. In particular, at low pressures it is possible to observe the minor isotopic species $^{13}CH_4$ in the presence of the most abundant $^{12}CH_4$ isotope (mixing ratio 1:100), as illustrated in Fig. 4. The mixing ratio is not given directly by the observed intensity relation, since the studied lines do not originate from the same energy levels, but in principle, knowing the relative oscillator strength it is possible to deduce the exact mixing ratio.

After this demonstration of DFG spectroscopy we want to focus on the main theme of this work, namely the simultaneous detection of O_2, H_2O and CH_4. Simultaneous recordings of the three species are shown in Fig. 5 for the 15-m open-air path length in the laboratory, together with computed spectra from the HITRAN molecular spectroscopic database [20]. The figure shows the single O_2 A-band line, R7Q8, the single H_2O $5_{33} \leftarrow 6_{34}$ line in the $\nu_1 + 2\nu_2 + \nu_3$ water band and a portion of the CH_4 P-branch of the fundamental ν_3 me-

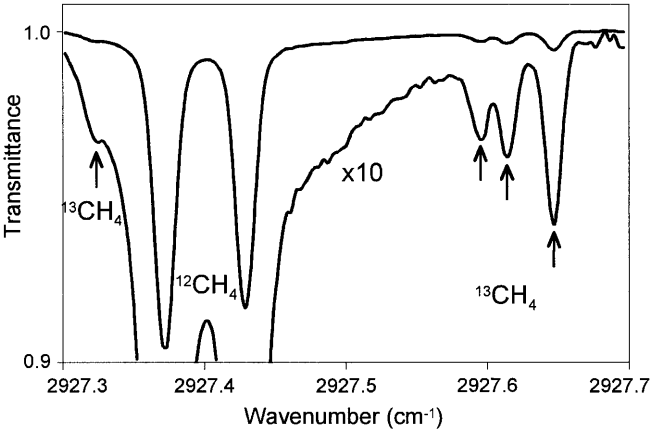

Fig. 4. Low-pressure recording of methane gas exhibiting the low-abundance species $^{13}CH_4$ in the presence of the normal $^{12}CH_4$ isotope

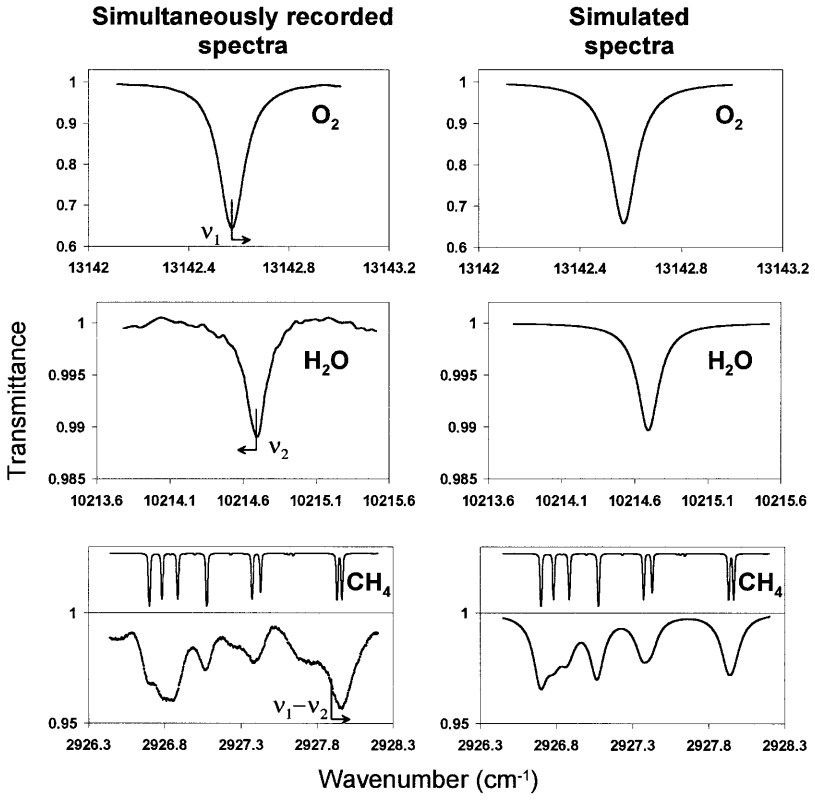

Fig. 5. Simultaneous recordings of oxygen, water vapour and methane in a 15-m atmospheric path and corresponding spectral simulations based on HITRAN. Recording time is 4.5 s. Scan directions in the individual laser sweeps and for the difference-frequency recording are indicated. Low-pressure, high-resolution spectra are included in the methane data

thane band. By recording the whole oxygen and water profiles, and by scanning the frequency of the two diode lasers in opposite directions, a total frequency scan of 3.6 cm^{-1} is obtained in the mid infrared. We choose to show 1.8 cm^{-1} of the scanned region where methane has prominent absorption lines. One can observe that the atmospheric-pressure methane experimental and theoretical curves show some deviations not present in the low-pressure short-path-length data. We conclude that the deviations can then not be due to some spurious laser mode running. The residual non-methane spectrum is most likely due to a low concentration of some interfering non-identified indoor-environment hydrocarbon. We do not believe that the deviations are due to etalon fringes, since the structure is insensitive to small adjustments of the optical components, and fringes were ascertained to be absent in independent measurements.

CH_4 has an outdoor background atmospheric abundance of 1.7 ppm, and a somewhat higher concentration in the indoor air is expected. By fitting non-interfering experimental methane lines with Lorentzian lineshapes, we have deduced that the typical methane background concentration in our laboratory is 3 ppm. With an observed signal-to-noise ratio (SNR) of about 20 in our recorded spectra at atmospheric pressure, we conclude that sensitivity in the 150-ppb range is achievable. The SNR was calculated as the ratio of the absorption-peak value and the peak-to-peak value of the noise. During our measurements the relative humidity of the air was fairly constant, ranging from 35% to 45%. On the day of the recording in Fig. 5, the relative humidity was measured to be 40% with a hygrometer (equivalent to 11 300-ppm H_2O). According to the observed SNR of 40, the detection limit for H_2O is 280 ppm. The normal O_2 concentration of 21% was measured and, as expected, this O_2-concentration value does not change at all from one day to another. The SNR in the O_2 recording was approximately 1300, indicating a detection limit of 170 ppm.

As an example of recordings relevant to, e.g., the working environment, a 15-min sequence of concentration determinations is shown in Fig. 6, exhibiting the response to the release of methane from a gas tank. The close-lying CH_4 transitions at 2928 cm^{-1} shown to the right in the spectral recordings of Fig. 5 were used. Raw data from recordings of the pressure-broadened single-peak feature are shown as insets in the figure (0.9-s integration time). We note that the methane concentration is reduced to its background level after approximately 15 min. The structure occurring at 2 min was

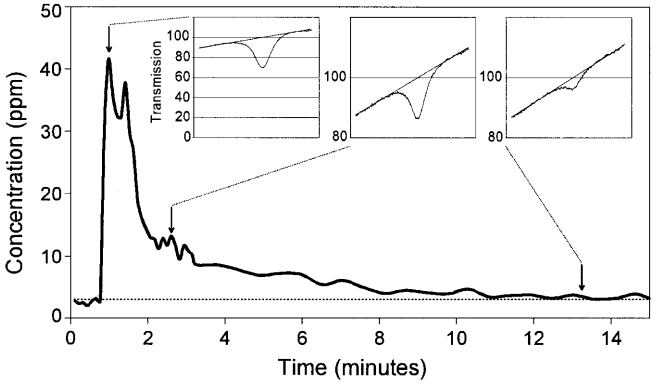

Fig. 6. Monitoring of indoor-methane concentration following the release of a small amount of gas from a tank. The measurement was performed over a 15-m path length. Raw-data spectral recordings are shown as *insets* in the figure

due to one of the authors walking around in the room, inducing turbulent mixing.

3 Conclusions

We have used two near-infrared diode lasers and difference-frequency generation in a periodically pooled lithium niobate crystal for simultaneous detection of oxygen at 760 nm, water vapour at 980 nm and methane at 3.4 μm. This is accomplished by probing each molecular species by the two near-infrared wavelengths and the generated mid-infrared wavelength, respectively. Recordings of atmospheric-pressure-broadened lines over a 15-m open path of laboratory air are demonstrated, and show the potential of the new measurement scheme for multispecies detection. Especially interesting is the possibility to simultaneously probe mid-infrared-absorbing molecular species and near-infrared-absorbing molecules without strong mid-infrared absorption. A continuous tuning range in the mid infrared of $3.6\,\mathrm{cm}^{-1}$ is achieved by synchronously scanning the frequency of both near-infrared lasers. Isotopic-species detection and pressure-dependence studies of methane lineshapes were performed in an absorption cell. A typical indoor-air methane background level of 3 ppm was reported, which as expected is higher than the typical outdoor level of 1.7 ppm. The signal-to-noise ratio in the recorded methane spectra indicates that sub-ppm detection of methane at atmospheric pressure is feasible over a measurement path of 10 m, and that practical multispecies detection can be performed over longer outdoor absorption paths.

Acknowledgements. The absorption-wavelength relations for multispecies monitoring were pointed out by Dr. V.S. Avetisov. This work was supported by the Swedish Research Council for Engineering Sciences (TFR) and the Knut and Alice Wallenberg Foundation.

References

1. A.A. Kosterov, R.F. Curl, F.K. Tittel, G. Gmachl, F. Capasso, D.L. Sivco, J.N. Baillargeon, A.L. Hutchinson, A.Y. Cho: Opt. Lett. **24**, 1762 (1999)
2. S.W. Sharpe, J.F. Kelly, J.S. Hartman, C. Gmachl, F. Capasso, D.L. Sivco, J.N. Baillargeon, A.Y. Cho: Opt. Lett. **23**, 1396 (1998)
3. K. Namjou, S. Cai, E.A. Whittaker, J. Faist, C. Gmachl, F. Capasso, D.L. Sivco, A.Y. Cho: Opt. Lett. **23**, 219 (1998)
4. U. Simon, C.E. Miller, C.C. Bradley, R.G. Hulet, R.F. Curl, F.K. Tittel: Opt. Lett. **18**, 1062 (1993)
5. K.P. Petrov, L. Goldberg, W.K. Burns, R.F. Curl, F.K. Tittel: Opt. Lett. **21**, 86 (1996)
6. W. Schade, T. Blanke, U. Willer, C. Rempel: Appl. Phys. B **63**, 99 (1996)
7. B. Sumpf, T. Kelz, M. Nägele, H.-D. Kronfeldt: Appl. Phys. B **64**, 521 (1997)
8. K.P. Petrov, S. Waltman, E.J. Dlugokencky, M. Arbore, M.M. Fejer, F.K. Tittel, L.W. Hollberg: Appl. Phys. B **64**, 567 (1997)
9. K.P. Petrov, R.F. Curl, F.K. Tittel: Appl. Phys. B **66**, 531 (1998)
10. D.G. Lancaster, D. Richter, R.F. Curl, F.K. Tittel: Appl. Phys. B **67**, 339 (1998)
11. M. Seiter, D. Keller, M.W. Sigrist: Appl. Phys. B **67**, 351 (1998)
12. T. Kelz, A. Schumacher, M. Nägele, B. Sumpf, H.-D. Kronfeldt: J. Quant. Spectrosc. Radiat. Transfer **61**, 591 (1999)
13. D.G. Lancaster, D. Richter, R.F. Curl, F.K. Tittel, L. Goldberg, J. Koplow: Opt. Lett. **24**, 1744 (1999)
14. U. Westblom, M. Aldén: Appl. Opt. **28**, 2592 (1989)
15. U. Westblom, M. Aldén: Appl. Spectrosc. **44**, 881 (1990)
16. D.S. Baer, R.K. Hanson, M.E. Newfield, N.K.J.M. Gopal: Opt. Lett. **19**, 1900 (1994)
17. M. Aldén, H. Edner, S. Svanberg: Appl. Phys. B **29**, 93 (1982)
18. B.J. Jefferies, R.A. Copeland, G.P. Smith, D.R. Crosley: Twentyfirst International Symposium on Combustion (The Combustion Institute, Pittsburg 1986) p. 1709
19. T.-B. Chu, M. Broyer: J. Phys. **46**, 523 (1985)
20. L.S. Rothman, C.P. Rinsland, A. Goldman, S.T. Massie, D.P. Edwards, J.-M. Flaud, A. Perrin, C. Camy-Peyret, V. Dana, J.-Y. Mandin, J. Schroeder, A. McCann, R.R. Gamache, R.B. Wattson, K, Yoshino, K.V. Chance, K.W. Jucks, L.R. Brown, V. Nemtchinov, P. Varanasi: J. Quant. Spectrosc. Radiat. Transfer **60**, 665 (1998)